Journal of
Emerging Investigators

Peptidomimetics Targeting the Polo-box Domain of Polo-like Kinase 1

Jihoon Jang[1], Terrence R. Burke Jr.[2], and David Hymel[2]

[1]Poolesville High School, Poolesville, MD

[2]Chemical Biology Laboratory, National Cancer Institute at Frederick, Frederick, MD

Summary

Polo-like kinase 1 (Plk1) is a master regulator of mitosis, activating key proteins that are involved in processes such as spindle assembly, centrosome maturation, and anaphase regulation. Certain types of cancers, including breast and stomach cancers, rely heavily on Plk1 overexpression for their growth and proliferation. Therefore, Plk1 is being investigated as a target for cancer drugs. Efforts to inhibit Plk1 have focused on the development of ATP-competitive small molecules directed at the kinase domain; however, these compounds can have dose-limiting toxicities attributed to off-target inhibition. Alternatively, peptide-based ligands targeted to the C-terminal polo-box domain (PBD) can inhibit the proper localization of Plk1, resulting in disrupted kinase activity and mitotic arrest. Here we synthesized and evaluated peptides and peptidomimetics derived from proteins known to interact with Plk1, which include polo-box interacting protein 1 (PBIP1), 205-kDa microtubule-associated protein (Map205), and budding uninhibited by benzimidazoles 1 (BUB1). Of these three proteins, sequences targeting Plk1 from Map205 and BUB1 have not previously been explored for structure-activity relationships. Our results show that analogs of all three proteins have modest binding activity with Plk1, confirming that Map205 and BUB1 are a new source of peptide ligands. Further development of these sequences could lead to high-affinity peptidomimetic ligands that could selectively induce mitotic arrest in cancer cells.

Received: January 22, 2016; **Accepted:** June 2, 2016; **Published:** August 19, 2016

Introduction

Human polo-like kinase 1 (Plk1) is a single polypeptide chain of 603 amino acids and has homologs in nearly all eukaryotic organisms (1). Its structure consists of a kinase domain (KD) at the N-terminus, as well as a highly conserved "polo-box domain" (PBD) composed of two polo-boxes near the C-terminus (**Figure 1**). The

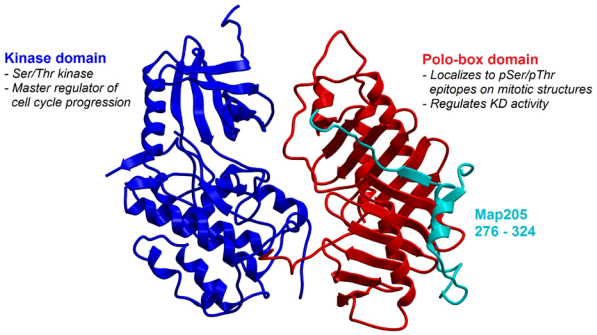

Figure 1: Structural domains of polo-like kinase 1 (Plk1). The X-ray co-crystal structure of the kinase and polo-box domains of Plk1 (*D. rerio*) bound to residues 296–324 of the 205-kDa microtubule-associated protein (Map205, *D. melanogaster*) illustrate the structural domains of Plk1 and their respective roles in cell-cycle regulation (PDB code: 4J7B).

PBD is involved in the regulation of kinase activity (2). As a master regulator of mitosis, Plk1 performs important functions such as activating and phosphorylating proteins involved in the maturation of centromeres, the formation of bipolar spindle fibers, and the regulation of anaphase (3, 4). Due to its role in initiating mitosis, Plk1 is overexpressed in certain types of cancers, including breast and stomach cancer (5). Biochemical inhibition of Plk1 using RNAi was shown to cause apoptosis in various cancer models, both *in vitro* and *in vivo* (6-8). Consequently, Plk1 has become a relevant target for potential anti-cancer drugs (9). By blocking the kinase activity of Plk1, such drugs are designed to halt mitosis in cancerous cells, which are dependent on Plk1 activity, while sparing normal and healthy cells (10). Several small molecule inhibitors targeting the ATP-binding site of the kinase domain have advanced to clinical trials, with some demonstrating clinical efficacy. However, many of these compounds have dose-limiting toxicities attributed to off-target inhibition. Strategies to target the kinase domain of Plk1 have been recently reviewed (11).

A major focal point in Plk1 research is the role of the PBD, as well as its value as a target for cancer drugs. The PBD is a highly conserved region in Plk1 that is critical for localization and specificity of its kinase activity (3). A single mutation within the PBD can lead to cells being unable to progress into mitosis, thus stalling cell division (12). Due to the highly conserved nature of this region,

the mutation most likely results in a loss of function of the PBD leading to the inability of Plk1 to activate key cell division proteins. Therefore, high-affinity ligands that specifically bind the PBD could potentially effectively inhibit Plk1 and halt mitosis (13). Given the uniqueness of the PBD, in contrast to the ubiquity of ATP-dependent kinases, agents that target the PBD are likely to be highly selective for Plk1, thus reducing the potential for off-target effects (14, 15).

Most published peptide-based Plk1 PBD–binding inhibitors are based on the amino acid sequence PLHSpT, a pentapeptide derived from polo-box interacting protein 1 (PBIP1) (16) (**Figure 2A**). Some analogs are able to bind to the PBD with nanomolar affinity, suggesting that these compounds could halt mitosis at very low concentrations. However, these peptides contain a critical phosphothreonine (pThr) residue, which reduces

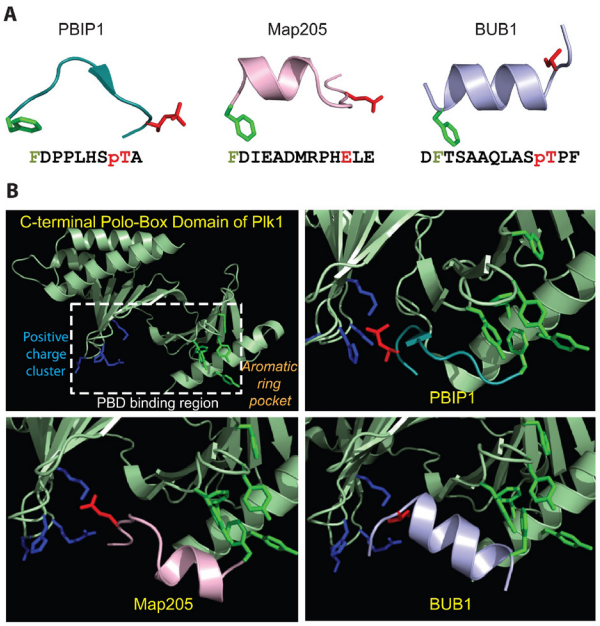

Figure 2: Structures of the peptidomimetics and the polo-box domain (PBD) of polo-like kinase 1 (Plk1). (**A**) Structures of polo-box interacting protein 1 (PBIP1, extracted from PBD code: 3P37), 205-kDa microtubule-associated protein (Map205, extracted from PDB code: 4J7B), and budding uninhibited by benzimidazoles 1 (BUB1, computationally predicted). The Glu or pThr residues are highlighted in red, and the Phe residues are highlighted in green. (**B**) Structures of the Plk1 PBD (top left panel) in complex with peptides derived from PBIP1 (top right panel), Map205 (bottom left panel), and BUB1 (bottom right panel). Peptides that mimic these regions are hypothesized to bind to the PBD. The Glu or pThr residues involved in the electrostatic interaction with Plk1 are highlighted in red, while the Phe residues involved in pi-stacking in the aromatic rich pocket of Plk1 are highlighted in green. The cartoons illustrate the crystal structures of Plk1 with PBIP1 (PDB code: 3P37) and Map205 (PDB code: 4J7B). The complex of PBD with the predicted BUB1 structure was computationally modeled.

their ability to penetrate through the cell membranes. Although several attempts have been made to optimize analogs of this pentapeptide in order to increase membrane permeability while maintaining binding affinity, these efforts have not yet produced a compound with potent activity in whole cells. The discovery of peptides derived from other sources may lead to new sequences that could potentially be further optimized for cell permeability and Plk1 selectivity, and thereby be effective in halting mitosis in cancer cells. Two candidates for this type of manipulation are the 205-kDa microtubule-associated protein (Map205), a Drosophila protein that has been co-crystallized with zebrafish Plk1 (17), and budding uninhibited by benzimidazoles 1 (BUB1), a human protein that interacts with Plk1 (18) (**Figure 2A**). Both of these proteins are able to bind to the PBD (**Figure 2B**), and aspects of their binding regions have similar three-dimensional structures as PBIP1, in that they contain an anionic amino acid at the C-terminus as well as a Phe residue at the N-terminus. The anionic amino acid near the C-terminus interacts with the positively charged His538 and Lys540 residues in the PBD pThr-binding pocket (2), while the Phe residues are involved in pi-stacking interactions with an aromatic rich pocket in the PBD (**Figure 2B**). As detailed here, we have synthesized and evaluated the Plk1 PBD binding affinities of peptide sequences derived from PBIP1, Map205, and BUB1. To date, there have been no reports of the synthesis or evaluation of PBD-binding peptides derived from Map205 or BUB1.

Results

Peptide design through computational analysis

Through a literature review, computational analysis using the Peptiderive protocol provided by the ROSIE online server, and structural analysis using Molsoft ICM-Pro, we predicted that residues 304 to 316 of the Map205 sequence and residues 599 to 611 of the BUB1 sequence bound the PBD. Both of these regions contained either a Glu or pThr involved in electrostatic interactions with His538 and Lys540 of Plk1, as well as an α-helix that directed a Phe residue into the aromatic rich pocket. We synthesized analogs of the wild-type sequences (Map205-Short-1, Map205-Long-1, BUB-pThr-1), along with analogs containing residues that promote the formation of the Phe-directing α-helix in solution (Map205-D305E-I306A-1, Map205-D305E-I306A-pThr-1), stapling residues to further stabilize the α-helix (Map205-E307-R311-Staple-1, Map205-E305-D309-Staple-1, Map205-NtermE307-Staple-1), and/or Glu/pThr substitutions that potentially increase cellular penetration (Map205-pThr-1, PBIP1-SEPL-1, PBIP1-SEA-1, BUB1-T609E-1). Furthermore, we also

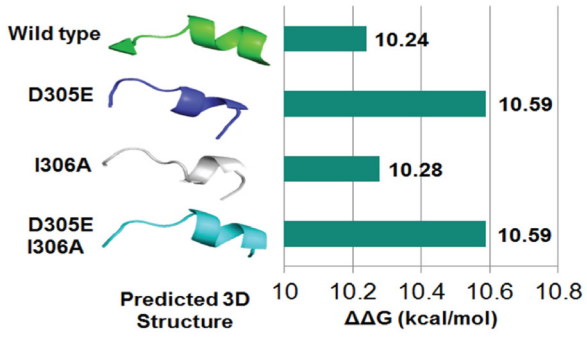

Figure 3: Predicted structure and ΔΔG values of the different combinations of D305E and I306A mutations for Map205 α-helix stabilization. An analog with both D305E and I306A mutations was predicted to generate the most stable α-helix while also maintaining a high ΔΔ*G* value. Using PEP-FOLD, the predicted 3-D structures of the three peptide analogs were generated and compared to the structure of the wild-type sequence of Map205. The results suggest that an analog with both D305E and I306A is predicted to form a peptide with a two-coil α-helix in solution. Using interface alanine scanning services provided by Robetta, we also predicted that these analogs would maintain a relatively high and constant ΔΔ*G* value, which indicates that binding affinity would not be lost due to these mutations.

synthesized mimetics of PBIP1 (from residues 71 to 79) with Pro-Leu residues substituted for Ala at residue 79 (PBIP1-SpTPL-1), due to literature demonstrating that a Pro-Leu motif could aid in binding (19).

The helix-promoting mutations proposed for the analogs of Map205 were evaluated using Robetta and PEP-FOLD. The results predicted that a combination of both the D305E and I306A mutations would be the most effective in promoting helix formation (**Figure 3**). The predicted 3D structures generated by PEP-FOLD indicated that both mutations would be needed for the peptide to form the two-coil α-helix found in the wild-type structure of Map205, while interface alanine scanning results from Robetta confirmed that the ΔΔ*G* value (the change in free energy) would be similar to the ΔΔ*G* value of wild-type Map205, suggesting that binding affinity would not be altered by the mutations. The X-ray co-crystal structure of the Map205 sequence bound to the PBD (PDB code: 4J7B) was used to guide the design of stapled peptides meant to lock the secondary structure of the resulting peptide. Residue pairs (*i* and *i*+4) at the solvent-exposed face of the α-helix were substituted for the non-natural amino acids propargylglycine (pG) and azidolysine (aK) to perform click-chemistry cyclizations (**Figure 4**). In total, 13 peptides and peptidomimetics were synthesized and tested (**Table 1**).

ELISA assay results

We used enzyme-linked immunosorbent assays (ELISA) to measure the binding affinity of Map205,

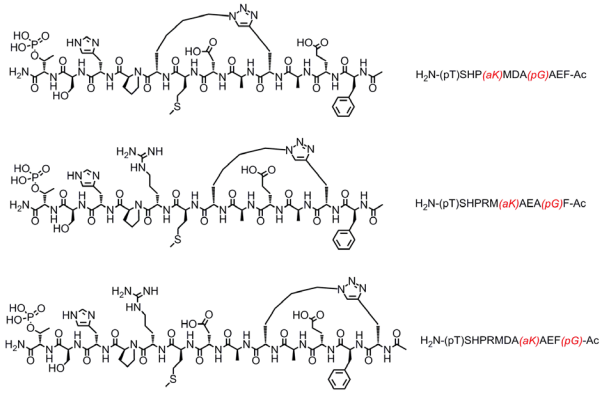

Figure 4: Chemical structure of the stapled peptides. Examples show Map205 peptides with mutations and staples.

BUB1, and PBIP1 peptidomimetic analogs with the PBD as well as full-length Plk1. The ELISA assays confirmed that analogs of Map205, PBIP1, and BUB1 are able to competitively bind to the PBD (**Figure 5**). Map205 analogs containing pThr (Map205-pThr) exhibited an IC_{50} value of 2.1 μM, whereas Map205 analogs containing pThr and the helix-promoting residues (Map205-D305E, I306A-pThr) exhibited an IC_{50} value of 4.9 μM (**Figure 5A**). One of the helix-stapled peptides, which substituted residues Glu305 and Asp309 for propargylglycine (pG) and azidolysine (aK), respectively, also exhibited modest activity with an IC_{50} value of 0.57 μM (**Figure 5B**). This latter compound was 3- to 8-fold more effective than the parent Map205 sequence. PBIP1 analogs and BUB1 analogs containing pThr showed activity as well. PBIP-SpTPL exhibited an IC_{50} value of 0.063 μM (**Figure 5C**); this was the most potent peptide generated, displaying slightly more activity than the wild-type sequence of PBIP1 (sequence of FDPPLHSpTA). Finally, the wild-type BUB1 sequence (BUB1-pThr) exhibited an IC_{50} value of 11 μM. All analogs of Map205, PBIP1, and

Peptide Name	Sequence	Rationale
Map205-Short-1	FDIEADMRPHE	Wild-type sequence of Map205
Map205-Long-1	FDIEADRMRPHELE	Wild-type sequence of Map205
Map205-pThr-1	FDIEADMRPH**SpT**	Glutamic Acid (E) → pThreonine (pT)
Map205-D305E-I306A-1	F**EA**EADMRPHE	Helix promoting substitutions
Map205-D305E-I306A-pThr-1	F**EA**EADMRPH**SpT**	E → pT; Helix prom subs
Map205-E307-R311-Staple-1	F**EA(pG)**ADM**(aK)**PH**SpT**	Stapled; Helix prom subs; E → pT
Map205-E305-D309-Staple-1	F**(pG)**AEA**(aK)**MRPH**SpT**	Stapled; Helix prom subs; E → pT
Map205-NtermE307-Staple-1	**(pG)**F**EA(aK)**ADMRPH**SpT**	Stapled; Helix prom subs; E → pT
PBIP1-SpTPL-1	FDPPLH**SpTPL**	Literature: SpTPL motif is effective
PBIP1-SEPL-1	FDPPLHSE**PL**	SpTPL motif + pT → E
PBIP1-SEA-1	FDPPLHSE**A**	SpTA motif; pT → E,
BUB1-pThr-1	DFTSAAQLA**SpT**PF	Wild-type sequence of BUB1
BUB1-T609E-1	DFTSAAQLASEPF	pT → E

Table 1: Final sequences of the synthesized peptides. Phosphothreonine residues are highlighted in red; the D305E/I306A mutations in Map205 are in green; the azidolysine (aK) and propargylglycine (pG) residues in stapled peptides are highlighted in purple and placed in parentheses.

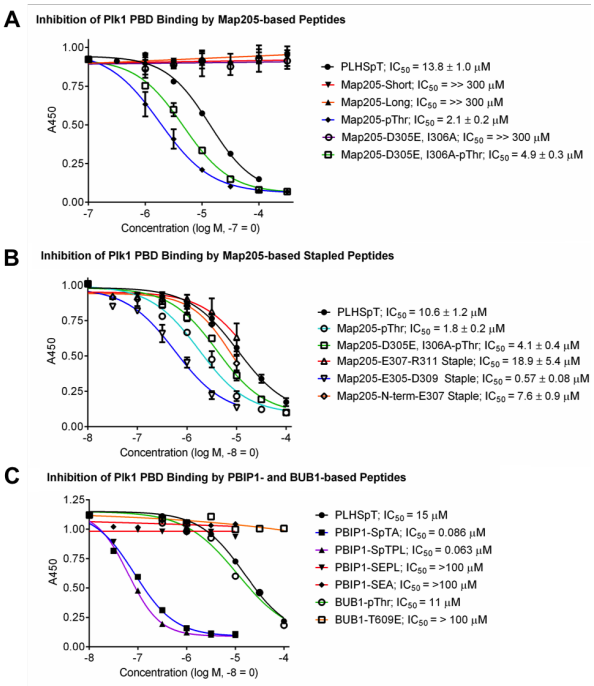

Figure 5: Results from the ELISA assays conducted against the polo-box domain (PBD) of polo-like kinase 1 (Plk1). Each ELISA assay was conducted under similar conditions and used a control pentapeptide (PLHSpT) for comparison. Assays for Map205-based peptides (**A** and **B**) were performed in duplicate (n=2, IC_{50} = average ± st. dev.), while assays of PBIP1- and BUB1-based peptides (**C**) were analyzed from single data points (n=1).

BUB1 that had pThr replaced by Glu did not show activity (IC_{50} values >300 μM), including the wild-type analogs of Map205 (Map205-Short, Map205-Long).

The most potent peptides were evaluated against full-length Plk1 (**Figure 6**). Assays using the full-length protein typically provided IC_{50} values that were approximately 10-fold less potent than with the isolated PBD, due to allosteric interactions between the KD and PBD. However, all five analogs examined against the full-length Plk1 had lower IC_{50} values than the control pentapeptide, PLHSpT, which is the current standard peptide for inhibiting the PBD of Plk1. The stapled peptide, Map205-E305-D309 Staple, had an IC_{50} value of 8.4 μM, and PBIP-SpTPL was the most active, with an IC_{50} value of 0.87 μM.

Discussion

We report the synthesis and evaluation of analogs of PBIP1, Map205, and BUB1 designed to target the PBD of Plk1. Analogs from all three proteins showed measurable binding affinities in ELISA assays that employed both the isolated PBD and full-length Plk1. Analogs from Map205 and BUB1 are particularly intriguing because they represent the first derivatives based on these proteins. The results show that

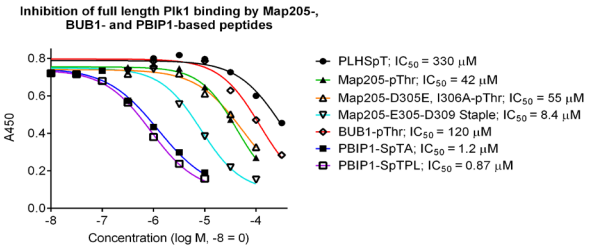

Figure 6: Inhibition of full-length Plk1 binding by Map205-, BUB1-, and PBIP1-based peptides. The most potent peptides from the polo-box domain (PBD) assays were tested by ELISA against the full-length protein. Single data points (n=1) were analyzed using non-linear regression to generate IC_{50} values.

sequences from Map205 and BUB1 could potentially be further developed into higher affinity ligands, similar to the development of peptidomimetic ligands based on PLHSpT. However, a new "starting point" other than the PBIP1 pentapeptide could potentially provide additional sources of peptidomimetic analogs that target the PBD of Plk1 (20).

In our experiments, we showed that PBIP1-SpTPL displays nanomolar affinity. Through optimization, this peptide could potentially be shortened and modified to yield analogs that are not only potent and selective for Plk1, but also cell permeable.

We also began optimizing the Map205 peptides by improving the helicity of these compounds. This optimization increased binding affinities 3- to 8-fold, presumably by directing the Phe residue into an aromatic-rich pocket on the protein surface, where pi-stacking interactions could occur. This observation supports the importance of the α-helix and pi-stacking interactions in binding to the PBD. It is highly likely that the parent sequences (Map205-pThr and Map205-D305E, I306A-pThr) have lower affinity due to a decreased ability to generate these pi-stacking interactions.

Of note, all analogs in which the pThr residue had been replaced by a Glu residue failed to show significant activity as compared to the corresponding pThr parents. It is a reasonable hypothesis that the tetrahedral shape and the di-anionic nature of the phosphoryl group allows it to be much more effective in interacting with the cationic amino acids of the PBD.

Future work will focus on increasing the binding affinities and cell permeabilities of these peptides. Further stapling of the α-helices may prove to be an effective approach to further boosting affinities by creating rigid helical structures that may better position the Phe residue for binding within the aromatic pocket. An alternate approach could be to eliminate the amino acid–based α-helix altogether by substituting a small molecule α-helix mimetic. By replacing coded amino acids with synthetic analogs, these constructs could

display improved affinities and cell permeabilities by decreasing the overall size and molecular weight of the compounds. Cell permeability could also be improved by finding a suitable substitution for the phosphothreonine residue. In using unexplored peptide sequences to discover new and potent compounds, this study may potentially provide new avenues of research to inhibit Plk1. Optimization of these ligands could lead to potent, selective, and cell permeable inhibitors of Plk1 for further pre-clinical development.

Methods

Design of peptides through computational analysis

The crystal structure of Map205 was analyzed to delineate the binding domain to be mimicked. A PDB file of the Map205-Plk1 binding complex (PDB code: 4J7B) was submitted to the Peptiderive Protocol on the ROSIE Online Server (http://rosie.rosettacommons.org/peptiderive) in order to calculate a possible binding region between the two proteins. The binding regions of PBIP1 (16) and BUB1 (18) have been published previously, so computational analysis was not necessary to identify the binding domain.

Analogs of the Map205 binding region consist of a critical α-helix that bends the peptide and directs a Phe residue into the aromatic rich pocket (**Figure 2B**). To stabilize this α-helix, amino acids within the sequence were substituted with helix-promoting residues. Asp305 and Ile306 were substituted with Glu and Ala, respectively. By substituting Asp with Glu, the negative charge is conserved; by substituting Ile with Ala, the hydrophobicity is conserved. Different combinations of the D305E and I306A mutations were evaluated. The structures of the analog with the D305E, I306A, and D305E-I306A mutations were predicted using PEP-FOLD (http://bioserv.rpbs.univ-paris-diderot.fr/services/PEP-FOLD/; 21, 22) and were compared to the structure of the wild-type Map205. In addition, the changes in free energy, $\Delta\Delta G$, of the analogs in complex with the PBD were calculated using interface alanine scanning (23) services provided by Robetta (http://robetta.bakerlab.org/). The $\Delta\Delta G$ due to alanine substitutions was calculated for both the complex and each partner using the equation

$$\Delta\Delta G = \Delta G^{Ala} - \Delta G^{WT}$$
$$= \left(\Delta G^{Ala}_{Complex} - \Delta G^{Ala}_{PBD} - \Delta G^{Ala}_{Peptide}\right)$$
$$-\left(\Delta G^{WT}_{Complex} - \Delta G^{WT}_{PBD} - \Delta G^{WT}_{Peptide}\right)$$

where *Ala* and *WT* denote the alanine mutation and wild-type protein, respectively, and $\Delta G_{Complex}$, ΔG_{PBD}, and $\Delta G_{Peptide}$ are the stabilities of the complex, the PBD, and the Map205 peptide, respectively. The free energy calculations confirm that mutations in Asp305 and Ile306 do not have an effect on the binding free energy (24).

Solid-phase peptide synthesis

All peptide analogs were synthesized from the C-terminus to the N-terminus using solid-phase peptide synthesis with Fmoc-protected amino acids. Synthesis was conducted in polypropylene columns containing a porous polyethylene disc filter. Rink amide AM resin was placed into the column, swelled in 2 mL of N,N-dimethylformamide (DMF), and placed on a shaker for 30 minutes. Fmoc deprotection was done with 3 mL of 20% piperidine in DMF with shaking for 10 minutes (2x). Concurrently, 4 equiv. of amino acid in 3 mL of DMF with 8% diisopropylethylamine (DIEA) were pre-activated with 3.95 equiv. of 1-[bis(dimethylamino) methylene]-1H-1,2,3-triazolo[4,5-b]pyridinium 3-oxid hexafluorophosphate (HATU) for at least 5 minutes. The resin was washed 4x with 3 mL of DMF. The pre-activated amino acid mixture was then added to the column and placed on the shaker. For the coupling of the first amino acid, the resin was shaken for at least 8 hours in order to ensure complete coupling; all other couplings were shaken for at least 3 hours. This procedure was repeated until all amino acids were introduced.

After the final amino acid was coupled and the column was washed and deprotected, the peptide was acetylated at the N-terminus by shaking with 3 mL of a 1:1:5 solution of acetic anhydride:DIEA:DMF for 30 minutes. Subsequently, the resin was washed 4x with DMF and 4x with dichloromethane (DCM). Peptides were then cleaved from the resin by treating with 3 mL of 95% trifluoroacetic acid (TFA), 2.5% triisopropylsilane (TIPS), and 2.5% H_2O for 2 h. Peptides containing a pThr residue required longer reaction times (at least 4 h) to ensure the deprotection of the phosphate O-benzyl protecting group. After shaking, the TFA solution was collected and washed with a small volume (approximately 0.5 mL) of DCM. Ice-cold diethyl ether was poured directly into the TFA solution to precipitate the peptide and 50 mL conical tubes containing the precipitated solution were centrifuged at 4°C for 5 minutes at 5000 G. The supernatant was discarded, and the peptide pellet was collected and dissolved in a solution of 50% acetonitrile (MeCN) in H_2O and purified using preparative reverse-phase HPLC (H_2O/MeCN gradient elution and UV monitoring at 215 nm). The purified fractions were verified using LC-MS and lyophilized for storage.

Stapling the peptides through click chemistry

The α-helical regions of select peptides were "stapled" by click cyclization of the non-natural amino acids azidolysine and propargyl-glycine (**Figure 4**). Peptides were stapled at positions 307 and 311, 305 and 309, or

between the N-terminus and 307. Fmoc-propargylglycine was purchased commercially, and fmoc-azidolysine was synthesized following a published procedure (25). The solid-phase peptide synthesis of these stapled analogs was slightly revised by using 3 equiv. of azidolysine and 2.5 equiv. of propargylglycine. Following cleavage and purification, the unstapled peptides underwent the click cyclization reactions, in which 2–3 mg of the peptide were dissolved in 50% dimethyl sulfoxide (DMSO) in H_2O. To this was added a mixture of 0.5 equiv. of $CuSO_4$ (4% w/v in H_2O), 0.6 equiv. of tris(3-hydroxypropyltriazolylmethyl) amine (THPTA) (from 100 mM in DMSO), and 5 equiv. of sodium ascorbate (from 0.5 M in H_2O), and the mixture was kept at room temperature for 48 h. A successful click reaction was confirmed by a shift in the retention time of an analytical HPLC trace. The peptide solution was then purified by semi-preparative reverse-phase HPLC and lyophilized for storage.

Evaluation of Plk1-binding affinities using an ELISA assay

The synthesized peptides were evaluated for Plk1-binding using competitive enzyme-linked immunosorbent assays (ELISA) assays, which employed an immobilized PBD-binding phosphopeptide. HEK-293T cells were transfected with plasmids encoding myc-tagged isolated Plk1 PBD or full-length Plk1. Cells were lysed by repetitive freeze/thaw cycles while suspended in a lysis buffer (PBS pH 7.4 with 0.5% NP-40, plus a protease and phosphatase inhibitor cocktail). In order to determine the total protein concentration in the lysates, bicinchoninic acid (BCA) assays were conducted using a standard BCA Assay Kit (Thermo Fisher Scientific Inc.). The lysate was diluted in PBS plus protease and phosphatase inhibitors to 300 µg/mL. Separately, a biotinylated-PBD binding phosphopeptide in PBS (1 µM) was added to a streptavidin-coated ELISA plate and shaken (1 h). The plate was then washed with PBS plus 0.05% Tween-20 (PBST) before being blocked with 1% bovine serum albumin (BSA) and shaken (1 h). Synthetic peptides were serially diluted in a separate plate, combined with the lysate, and added to the ELISA plate and shaken (1 h). After washing 4x with PBST, the primary antibody (anti-myc, 1:1500 dilution in PBS) was added and shaken (1 h). After another 4x-wash with PBST, the secondary antibody (rabbit anti-mouse HPR-conjugate, 1:3000 dilution in 1% BSA in PBS) was added and shaken (1 h). Finally, after washing with PBST (5x) 3,3',5,5'-tetramethylbenzidine (TMB) substrate was added and shaken for 5 to 10 minutes before being quenched with a 2N H_2SO_4 stop solution. The plate was then read for absorbance at 450 nm with a BioTek Synergy 2 plate reader. Absorbance was normalized and plotted versus concentration, then analyzed using non-linear regression analysis in GraphPad Prism 6 to generate IC_{50} values. When possible, experiments were performed in duplicate and analyzed in a similar manner to provide IC_{50} values as average ± standard deviation.

Acknowledgements

This work was supported in part by the Intramural Research Program of the NIH, Center for Cancer Research, National Cancer Institute, National Institutes of Health. The content of this publication does not necessarily reflect the views or policies of the Department of Health and Human Services, nor does the mention of trade names, commercial products, or organizations imply endorsement by the U.S. Government.

References

1. Holtrich, U., G. Wolf, A. Brauninger, T. Karn, B. Bohme, H. Rubsamen-Waigmann, and K. Strebhardt. 1994. "Induction and down-regulation of PLK, a human serine/threonine kinase expressed in proliferating cells and tumors." *Proc Natl Acad Sci* 91:1736-1740.
2. Cheng, K. Y., E. D. Lowe, J. Sinclair, E. A. Nigg, and L. N. Johnson. 2003. "The crystal structure of the human polo-like kinase-1 polo box domain and its phospho-peptide complex." *EMBO J* 22:5757-5768.
3. Elia, A. E., P. Rellos, L. F. Haire, J. W. Chao, F. J. Ivins, K. Hoepker, D. Mohammad, L. C. Cantley, S. J. Smerdon, and M. B. Yaffe. 2003. "The molecular basis for phosphodependent substrate targeting and regulation of Plks by the Polo-box domain." *Cell* 115:83-95.
4. van Vugt, M. A., and R. H. Medema. 2005. "Getting in and out of mitosis with Polo-like kinase-1." *Oncogene* 24:2844-2859.
5. Degenhardt, Y., and T. Lampkin. 2010. "Targeting Polo-like kinase in cancer therapy." *Clin Cancer Res* 16:384-389.
6. Guan, R., P. Tapang, J. D. Leverson, D. Albert, V. L. Giranda, and Y. Luo. 2005. "Small interfering RNA-mediated Polo-like kinase 1 depletion preferentially reduces the survival of p53-defective, oncogenic transformed cells and inhibits tumor growth in animals." *Cancer Res* 65:2698-2704.
7. Spankuch, B., Y. Matthess, R. Knecht, B. Zimmer, M. Kaufmann, and K. Strebhardt. 2004. "Cancer inhibition in nude mice after systemic application of U6 promoter-driven short hairpin RNAs against PLK1." *J Natl Cancer Inst* 96:862-872.
8. Spankuch, B., I. Steinhauser, H. Wartlick, E. Kurunci-Csacsko, K. I. Strebhardt, and K. Langer. 2008. "Downregulation of Plk1 expression by receptor-mediated uptake of antisense oligonucleotide-loaded nanoparticles." *Neoplasia* 10:223-234.
9. Strebhardt, K., and A. Ullrich. 2006. "Targeting polo-

like kinase 1 for cancer therapy." *Nat Rev Cancer* 6:321-330.

10. Lapenna, S., and A. Giordano. 2009. "Cell cycle kinases as therapeutic targets for cancer." *Nat Rev Drug Discov* 8:547-566.
11. Lee, K. S., T. R. Burke, Jr., J. E. Park, J. K. Bang, and E. Lee. 2015. "Recent Advances and New Strategies in Targeting Plk1 for Anticancer Therapy." *Trends Pharmacol Sci* 36:858-877.
12. Lee, K. S., T. Z. Grenfell, F. R. Yarm, and R. L. Erikson. 1998. "Mutation of the polo-box disrupts localization and mitotic functions of the mammalian polo kinase Plk." *Proc Natl Acad Sci* 95:9301-9306.
13. Qian, W., J. E. Park, F. Liu, K. S. Lee, and T. R. Burke, Jr. 2013. "Effects on polo-like kinase 1 polo-box domain binding affinities of peptides incurred by structural variation at the phosphoamino acid position." *Bioorg Med Chem* 21:3996-4003.
14. McInnes, C., K. Estes, M. Baxter, Z. Yang, D. B. Farag, P. Johnston, J. S. Lazo, J. Wang, and M. D. Wyatt. 2012. "Targeting subcellular localization through the polo-box domain: non-ATP competitive inhibitors recapitulate a PLK1 phenotype." *Mol Cancer Ther* 11:1683-1692.
15. Liu, X. 2015. "Targeting Polo-Like Kinases: A Promising Therapeutic Approach for Cancer Treatment." *Transl Oncol* 8:185-195.
16. Yun, S. M., T. Moulaei, D. Lim, J. K. Bang, J. E. Park, S. R. Shenoy, F. Liu, Y. H. Kang, C. Liao, N. K. Soung, S. Lee, D. Y. Yoon, Y. Lim, D. H. Lee, A. Otaka, E. Appella, J. B. McMahon, M. C. Nicklaus, T. R. Burke, Jr., M. B. Yaffe, A. Wlodawer, and K. S. Lee. 2009. "Structural and functional analyses of minimal phosphopeptides targeting the polo-box domain of polo-like kinase 1." *Nat Struct Mol Biol* 16:876-882.
17. Xu, J., C. Shen, T. Wang, and J. Quan. 2013. "Structural basis for the inhibition of Polo-like kinase 1." *Nat Struct Mol Biol* 20:1047-1053.
18. Qi, W., Z. Tang, and H. Yu. 2006. "Phosphorylation- and polo-box-dependent binding of Plk1 to Bub1 is required for the kinetochore localization of Plk1." *Mol Biol Cell* 17:3705-3716.
19. Elia, A. E., L. C. Cantley, and M. B. Yaffe. 2003. "Proteomic screen finds pSer/pThr-binding domain localizing Plk1 to mitotic substrates." *Science* 299:1228-1231.
20. Ahn, M., Y. H. Han, J. E. Park, S. Kim, W. C. Lee, S. J. Lee, P. Gunasekaran, C. Cheong, S. Y. Shin, Sr., H. Y. Kim, E. K. Ryu, R. N. Murugan, N. H. Kim, and J. K. Bang. 2015. "A new class of peptidomimetics targeting the polo-box domain of Polo-like kinase 1." *J Med Chem* 58:294-304.
21. Maupetit, J., P. Derreumaux, and P. Tuffery. 2010. "A fast method for large-scale de novo peptide and miniprotein structure prediction." *J Comput Chem* 31:726-738.
22. Maupetit, J., P. Derreumaux, and P. Tuffery. 2009. "PEP-FOLD: an online resource for de novo peptide structure prediction." *Nucleic Acids Res* 37:W498-503.
23. Kortemme, T., D. E. Kim, and D. Baker. 2004. "Computational alanine scanning of protein-protein interfaces." *Sci STKE* 2004:pl2.
24. Kortemme, T., and D. Baker. 2002. "A simple physical model for binding energy hot spots in protein-protein complexes." *Proc Natl Acad Sci* 99:14116-14121.
25. Park, J. H., and M. L. Waters. 2013. "Positional effects of click cyclization on beta-hairpin structure, stability, and function." *Org Biomol Chem* 11:69-77.